

# Lung-Specific mRNA Delivery Enabled by Sulfonium Lipid Nanoparticles

David O. Popoola,<sup>#</sup> Zhi Cao,<sup>#</sup> Yuqin Men, Xinyuan Li, Mariano Viapiano, Stephan Wilkens, Juntao Luo, Yong Teng, Qinghe Meng, and Yamin Li\*



Cite This: <https://doi.org/10.1021/acs.nanolett.4c01854>



Read Online

ACCESS |



Metrics & More



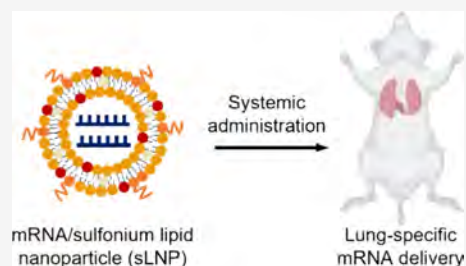
Article Recommendations



Supporting Information

**ABSTRACT:** Among various mRNA carrier systems, lipid nanoparticles (LNPs) stand out as the most clinically advanced. While current clinical trials of mRNA/LNP therapeutics mainly address liver diseases, the potential of mRNA therapy extends far beyond—yet to be unraveled. To fully unlock the promises of mRNA therapy, there is an urgent need to develop safe and effective LNP systems that can target extrahepatic organs. Here, we report on the development of sulfonium lipid nanoparticles (sLNPs) for systemic mRNA delivery to the lungs. sLNP effectively and specifically delivered mRNA to the lungs following intravenous administration in mice. No evidence of lung and systemic inflammation or toxicity in major organs was induced by sLNP. Our findings demonstrated that the newly developed lung-specific sLNP platform is both safe and efficacious. It holds great promise for advancing the development of new mRNA-based therapies for the treatment of lung-associated diseases and conditions.

**KEYWORDS:** Sulfonium lipid nanoparticle, mRNA delivery, lung targeting, pulmonary endothelium, genome engineering



mRNA therapeutics hold great promise in protein replacement therapy, gene editing, oncology, etc.<sup>1,2</sup> Lipid nanoparticles (LNPs) are the most clinically advanced delivery system for RNA drugs.<sup>3,4</sup> In addition to vaccines, LNP-enabled mRNA therapeutics are undergoing thorough investigation across various fields.<sup>5–9</sup> Despite the great efforts, the ongoing clinical trials of mRNA/LNP therapeutics mainly focus on liver-associated diseases. An efficacious LNP system that can target extrahepatic organs is the key to broadening the potential of mRNA therapeutics.<sup>8,10–12</sup>

Lung-targeted mRNA delivery is useful in treating various lung-associated diseases, such as cystic fibrosis and lung cancer.<sup>13–17</sup> LNPs have been employed for both local (e.g., inhalation, and intratracheal) and systemic (e.g., intravenous) delivery of mRNA to the lungs.<sup>18–23</sup> Local administration is straightforward and efficient, but when challenges arise (e.g., toxicity, irritative reactions, and patient inability), systemic delivery can be preferred.<sup>24,25</sup>

For systemic mRNA delivery to the lung, several LNP systems have been developed.<sup>26–29</sup> Kaczmarek et al. synthesized a library of polymer–lipid nanoparticles for the delivery of mRNA and DNA.<sup>30</sup> Their nanoparticles primarily delivered mRNA to the lungs following intravenous injection and a strong protein production was observed within 48 h postinjection. Cheng and colleagues reported a systematic approach for fabricating lung-targeting LNP systems.<sup>31</sup> Their versatile strategy incorporated a proper amount of cationic excipient lipid (e.g., DOTAP) into the four-component ionizable lipid-containing formulations, and results show

LNP redirection from the liver to the lungs after systemic injection. Later, LoPresti et al. demonstrated that simply replacing the helper phospholipid in the four-component LNP formulation with permanently charged cationic lipids also facilitates lung targeting.<sup>32</sup> More recently, Qiu et al. reported on a group of amide linker-containing LNPs for lung-selective delivery of mRNA and showed therapeutic effects in a mouse model of lymphangioleiomyomatosis.<sup>33</sup>

Continued efforts are essential for the development of novel, safe, and effective (LNP) systems tailored for lung-specific mRNA delivery. In this study, we report on the synthesis of a novel class of LNPs, namely sulfonium LNPs (sLNPs), constructed from sulfonium lipids, and investigate their potential for delivering mRNA systemically to the lungs. In contrast to conventional amine-based lipids, our newly developed lipids feature positively charged sulfonium groups for mRNA complexation and intracellular delivery. To the best of our knowledge, this represents the first documentation of sulfonium lipids and sLNP developed specifically for mRNA delivery and organ targeting. Our findings demonstrate that upon intravenous administration, the sLNPs efficiently and

**Received:** April 18, 2024

**Revised:** June 10, 2024

**Accepted:** June 10, 2024

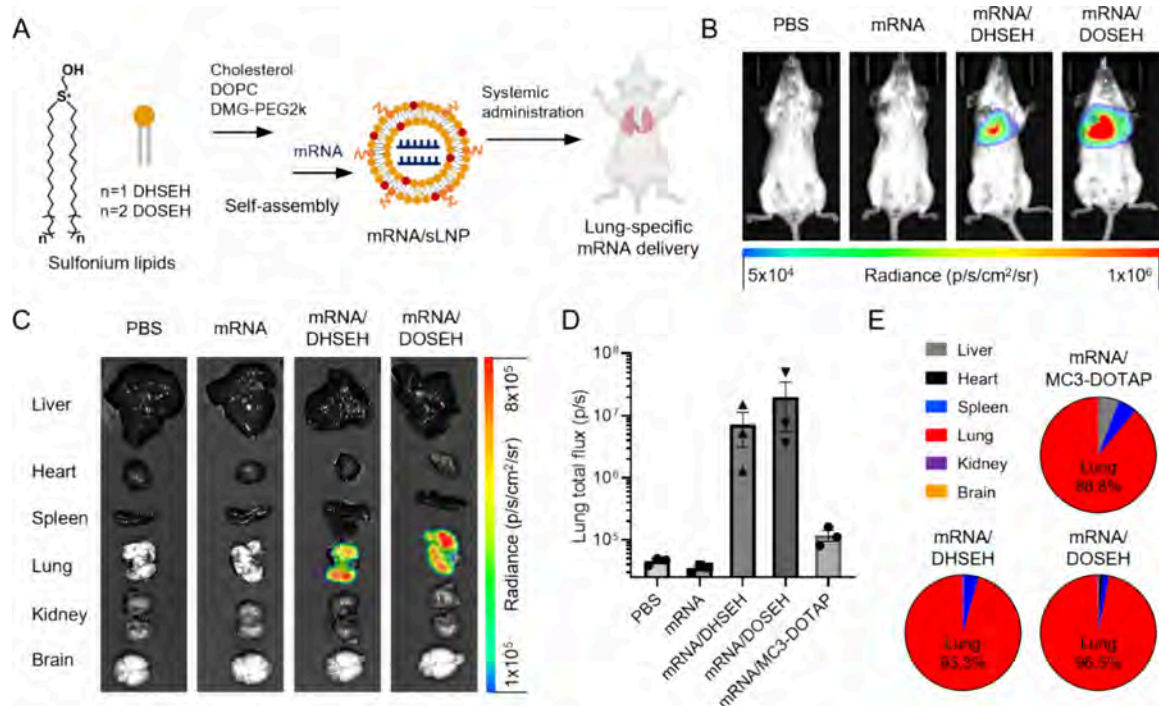


**Figure 1.** Sulfonium lipid nanoparticle (sLNP)-enabled systemic delivery of mRNA to the lungs. (A) Schematic illustration of the chemical structures of sulfonium lipids (DHSEH and DOSEH), the self-assembly process of mRNA-loaded sLNP (mRNA/sLNP), and the targeted delivery of mRNA to the lungs in mice. (B) Representative *in vivo* whole-body bioluminescence images of mice treated with PBS, free fLuc mRNA, and mRNA/sLNPs. (C) Representative *ex vivo* bioluminescence images of mouse organs. (D) Quantification of total bioluminescence flux from the lungs of mice treated with PBS, free mRNA, and mRNA-loaded LNPs. Data are presented as mean  $\pm$  s.e.m.,  $n = 3$ . (E) Percentage of background-subtracted bioluminescence signal originating from each organ in mice treated with mRNA-loaded LNPs.

safely deliver various types of mRNA to the lungs, leading to robust protein production (Figure 1A).

Sulfonium lipids, DHSEH and DOSEH were synthesized according to the procedure described in the Materials and Methods. Their chemical structures were characterized by <sup>1</sup>H NMR and MS (Figures S1 and S2).

The sLNPs containing sulfonium lipids (DHSEH or DOSEH), cholesterol, DOPC, and DMG-PEG2k were fabricated through self-assembly (Figure 1A).<sup>34–36</sup> The sulfonium lipids provide a matrix to incorporate other ingredients, and they can bind with mRNA molecules primarily through electrostatic interactions. Cholesterol is used to stabilize the supramolecular structure, tune the rigidity and fluidity of the lipid membrane, and promote cellular internalization. The helper phospholipids participate in the formation of the lipid bilayer and facilitate endosomal escape. PEG-lipid is used to improve colloidal stability by providing steric hindrance and nonfouling characteristics.

For the *in vivo* mRNA delivery study, fLuc mRNA was loaded into sLNPs (denoted as mRNA/DHSEH and mRNA/DOSEH). Balb/c mice received either PBS, free mRNA, or mRNA/sLNP (0.1 mg mRNA/kg body weight). Both mRNA/DHSEH and mRNA/DOSEH induced strong bioluminescence signals, suggesting successful mRNA delivery and protein production (Figure 1B). The observed signals primarily originate from the lungs. Previous studies have shown that positively charged LNPs tend to accumulate in the lungs following intravenous injection.<sup>37–40</sup> Dilliard et al. showed that a group of lung-specific LNPs shared similar apparent  $pK_a$  values of  $>9.25$ , suggesting that these LNPs possess net positive charges at physiological pH.<sup>41</sup> In another

study, Huang et al. showed that the quaternization of amine lipids redirected LNP from the spleen to the lungs.<sup>37</sup> No signals were recorded for mice injected with PBS or free mRNA (Figure 1B), indicating systemic administration of free mRNA cannot induce efficacious protein expression. Consistent with the *in vivo* imaging results, *ex vivo* bioluminescence signals were predominantly observed in the lungs of mice receiving mRNA/sLNPs (Figure 1C). The total bioluminescence emission flux from lungs was then quantified (Figure 1D). Lungs from mice receiving free mRNA (ca.  $3.49 \times 10^4$  p/s) showed a similar signal intensity compared to the PBS group (ca.  $4.51 \times 10^4$  p/s), further confirming the inefficiency of systemically injected free mRNA. mRNA/DHSEH led to  $\sim 200$ -fold intensity increase (ca.  $7.25 \times 10^6$  p/s) compared to the free mRNA group, and mRNA/DOSEH was more efficient, showing a 2.79-fold higher flux intensity compared with mRNA/DHSEH (ca.  $2.02 \times 10^7$  p/s). Notably, the mRNA/sLNP formulations exhibited stronger signals compared to the benchmark lung-targeting MC3-DOTAP LNPs (ca.  $1.18 \times 10^5$  p/s; Figure 1D and S3).<sup>27,31,42,43</sup> In terms of organ specificity (Figure 1E), it was found that ca. 95.3% and 96.5% bioluminescence signals originated from the lungs of mice administered with mRNA/DHSEH and mRNA/DOSEH sLNP, respectively, outperforming the MC3-DOTAP formulation (ca. 88.8%).

The physicochemical properties of mRNA/sLNP were then characterized. mRNA/DHSEH and mRNA/DOSEH showed average hydrodynamic diameters ( $\langle Dh \rangle$ ) of 243.6 and 188.3 nm, respectively (Figure S4A). Their sizes are in the optimal range for systemic circulation, as previous studies indicated that small nanoparticles (e.g.,  $< 10$  nm) could undergo renal

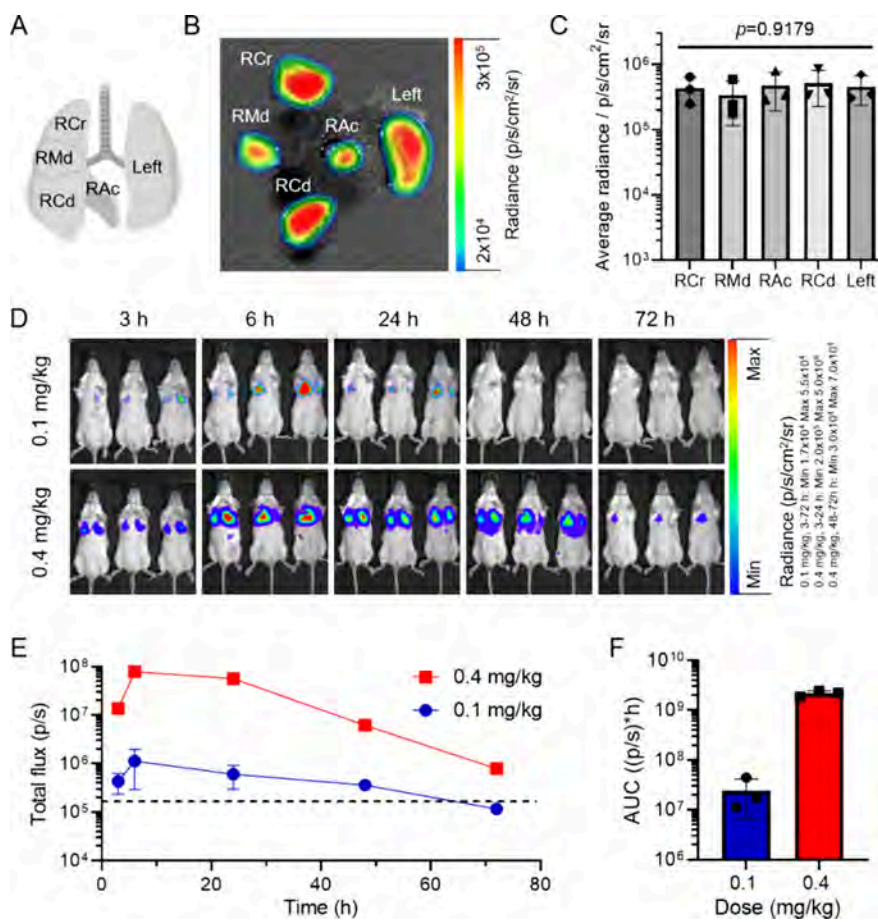


**Figure 2.** Distribution of protein expression and kinetics study of mRNA/sLNP. (A) Schematic illustration of mouse lung lobes. (B) Representative *ex vivo* bioluminescence images of dissected lung lobes. (C) Quantification of average radiance for all five lung lobes. Data are presented as mean  $\pm$  s.d.,  $n = 3$ , one-way ANOVA analysis. (D) Whole-body bioluminescence images and (E) quantification of total flux at different time points for high (0.4 mg/kg) and low doses (0.1 mg/kg). Data are presented as mean  $\pm$  s.d.,  $n = 3$ . (F) The area under the curve (AUC) analysis shows cumulative bioluminescence.

clearance, and big LNPs (e.g., > 400 nm) are prone to hepatic clearance.<sup>44,45</sup> It should be noted that, apart from the size, other physicochemical traits (e.g., surface charge and chemistry) all affect LNPs' behaviors.<sup>46,47</sup> Both mRNA/DHSEH (0.184) and mRNA/DOSEH (0.229) had a PDI lower than 0.3, implying their uniformity (Figure S4B). Both mRNA/DHSEH (42.52 mV) and mRNA/DOSEH (46.38 mV) were positively charged, attributing to the cationic sulfonium moieties (Figure S4C). The mRNA encapsulation efficacy was determined to be >99% for both DHSEH and DOSEH sLNPs (Figure S4D). We speculated that the cationic nature of sulfonium lipids and high positive charge density contributed to efficient mRNA binding. Finally, the morphology of sLNPs was examined using cryoEM. Both formulations showed a similar spherical liposomal structure, in which both unilamellar and multilamellar vesicles were observed (Figure S4E). Vesicles are one of the most common self-assembly structures of natural and synthetic lipids, and they have been extensively studied for the delivery of small molecule drugs, proteins, and nucleic acids.<sup>48</sup> Consistent with the well-studied siRNA/LNP systems, it was envisioned that the negatively charged mRNA molecules can bind to the inner and exterior lipid bilayer surfaces mainly through electrostatic interactions, and they can also be sandwiched between two layers of the multilamellar vesicles.<sup>49</sup> The physical complexation improves

the stability of mRNA molecules during systemic circulation and facilitates extravasation and cell internalization.

A common issue associated with the local drug administration to lungs is the suboptimal distribution of drugs.<sup>50,51</sup> In one study, locally administered viral vector-induced protein expression was primarily found in the nasal cavity, trachea, and proximal aspects of the lower respiratory tract.<sup>52</sup> Little to no protein production was found at the mid to distal aspects of lung lobes. Systemic delivery can potentially overcome this limitation as drugs are carried and distributed by systemic blood circulation. We dissected the lung lobes of Balb/c mice receiving fLuc mRNA/DOSEH (Figure 2A). All five lobes (i.e., right cranial (RCr), right middle (RMd), accessory (RAc), right caudal (RCd), and left) showed strong bioluminescence emission, and both the proximal and distal sites of primary bronchi had similar emission intensity (Figure 2B). Furthermore, bioluminescence radiance (p/s/cm<sup>2</sup>/sec) was quantified, and there was no significant difference between five lobes (Figure 2C). For kinetics study, fLuc mRNA/DOSEH was injected into Balb/c mice, and *in vivo* whole-body bioluminescence images were obtained at certain time intervals within 72 h (Figure 2D). At a dose of 0.1 mg mRNA/kg body weight, the signal gradually increased from 3 to 6 h (Figure 2E), and followed by a graduate decrease. No signals above the background were recorded at 72 h, indicating the exhaustion of delivered mRNA. This is comparable with the mRNA delivery

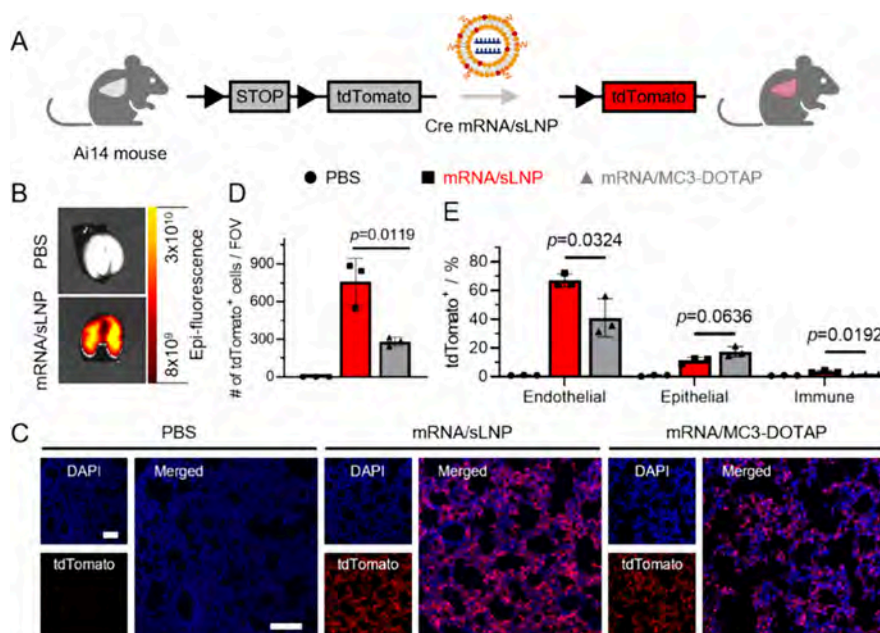


**Figure 3.** sLNP-mediated mRNA delivery for genome engineering in the mouse lungs. (A) Schematic illustration of Cre-Lox recombination and tdTomato activation in Ai14 mouse following successful Cre mRNA delivery. (B) Representative *ex vivo* fluorescence images of lungs. (C) Representative confocal images and (D) quantification of tdTomato-positive cells per field of view (FOV) of lung slices obtained from mice that received either PBS, Cre mRNA/sLNP, or Cre mRNA/MC3-DOTAP. Scale bar = 100  $\mu$ m. (E) Flow cytometry quantification of tdTomato-positive cells within lung endothelial, epithelial, and immune cell populations. Data are presented as mean  $\pm$  s.d.,  $n = 3$ , two-tailed unpaired  $t$  test.

kinetics observed for polymer–lipid nanoparticle D90-C12–103 reported in previous study.<sup>30</sup> We then speculated that a higher dose would induce longer and greater protein expression. At a dose of 0.4 mg mRNA/kg body weight, the signal peaked at 6 h, and then gradually decreased. At the end point of this experiment, 72 h, the emission signal was still above the background level. Mice were then sacrificed, and *ex vivo* organ imaging further confirmed bioluminescence emission from the lungs, and no signals were recorded for other organs (i.e., heart, liver, spleen, kidney; Figure S5). A consistent protein expression pattern further demonstrated the lung selectivity of our mRNA/sLNP system, as no obvious redistribution of delivered mRNA or encoded protein was found. The total protein production was calculated as the accumulated luminescence, and the 0.4 mg/kg group showed a ca. 90.4-fold higher protein production compared to the 0.1 mg/kg dose group (Figure 2F).

Next, we examined the possibility of using sLNP for the delivery of Cre recombinase mRNA for genome engineering in the lungs. Ai14 mice were used, which contain a loxP-flanked STOP codon upstream of the tdTomato reporter gene in its genome (Figure 3A).<sup>53</sup> Cre mRNA/DOSEH was administered to Ai14 mice (0.42 mg/kg), and lungs were harvested 5 days postinjection. Compared to the PBS-treated group, red fluorescence signals were observed in the lungs treated with Cre mRNA/sLNP (Figure 3B). Strong red fluorescence signals were recorded for both Cre mRNA/sLNP and the lung-tropic mRNA/MC3-DOTAP-injected mouse lung tissue slices (ca. 10  $\mu$ m), and tdTomato-positive cells were found to be present evenly in the lungs (Figure 3C). Further analysis revealed that sLNP induced approximately 2.69 times more tdTomato-positive cells/FOV, highlighting its high efficacy (Figure 3D). To further illustrate the identity of mRNA-transfected and tdTomato-positive cells in the lungs, single-cell suspensions were then prepared and stained with antibodies (i.e., anti-

CD31, anti-CD326, and anti-CD45) for flow cytometry analysis. It was revealed that ca. 67.0% endothelial cells, 11.3% epithelial cells, and 3.5% immune cells were successfully transfected (Figure 3E). Typical gating strategies for flow cytometry analysis are summarized (Figures S6 and S7). The lung-tropic MC3-DOTAP induced approximately 41.0%, 17.3%, and 1.7% tdTomato-positive endothelial, epithelial, and immune cells, respectively. While sLNPs and MC3-DOTAP showed similar efficiency in transfecting epithelial cells, sLNPs were significantly more effective in transfecting endothelial and immune cells in the lungs (Figure 3E). In the work by Qiu et al., 306-N16B transfected ca. 33.6% endothelial cells, 1.5% epithelial cells, and 1.9% immune cells.<sup>33</sup> Another formulation with 113-N16B transfected 69.6% endothelial cells, 7.3% epithelial cells, and 18.9% immune cells (0.75 mg mRNA/kg; day 7). Cheng et al. reported the efficiency of ca. 66% endothelial cells, 39% epithelial cells, and 21% immune cells in their SORT LNP study (0.3 mg/kg; day 2).<sup>31</sup> Furthermore, an estimated 22% endothelial cells, 4% epithelial cells, and 7% immune cells (0.6 mg/kg; day 2) were observed in a polymer-assisted five-element nanoparticle system developed by Cao et al.<sup>54</sup> Taken together, our findings indicated that the sLNP demonstrated a transfection efficacy in lung endothelial cells comparable to that of the benchmark lung-targeting LNPs. Furthermore, our results suggested that the sLNP displayed a higher specificity for endothelial cells, which could be advantageous in scenarios where the lung endothelium is the primary target for mRNA therapeutics delivery.<sup>55</sup>

It was expected that a protein corona would form on the surface of LNPs immediately after administration in the bloodstream.<sup>56</sup> Previous studies suggested a close relationship between the property of protein corona and LNPs' biodistribution profile. To identify the protein corona on sLNP, we incubated DOSEH sLNP with adult C57BL/6

mouse plasma and performed mass spectrometry proteomics analysis. A total of 245 different types of protein species were found adsorbed to DOSEH sLNP. The top ten most abundant proteins constitute ~52.3% of total proteins on the corona (Figure 4A). Among these adsorbed serum proteins, fibrinogen

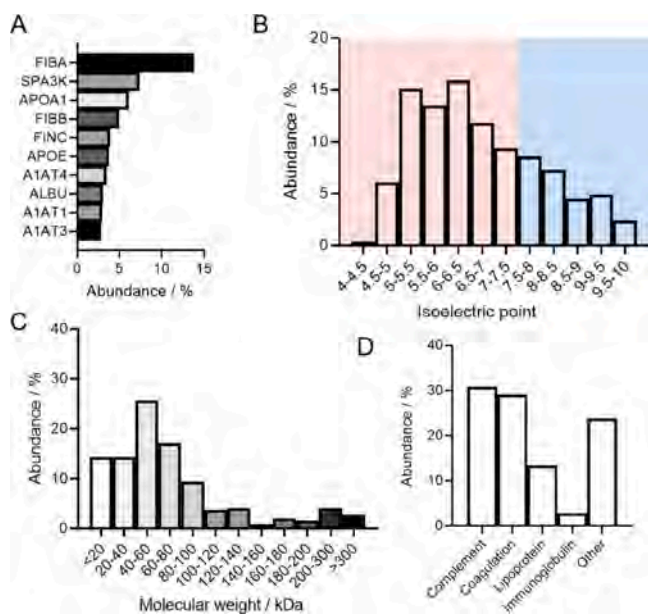


**Figure 4.** Proteomics analysis of sLNP protein corona. (A) Top 10 most abundant proteins on corona. The enriched proteins on the corona were categorized based on their (B) isoelectric point, (C) molecular weight, and (D) biological function.

alpha chain (FIBA), serine protease inhibitor A3K (SPA3K), and apolipoprotein A-1 (APOA1) are the top three. Since the sLNPs are positively charged, we envisioned plasma proteins with net negative charges under physiological pH could be more easily adsorbed onto sLNPs. It was found that ~72.2% of proteins possess a isoelectric point (PI) lower than 7.4, indicating the negatively charged proteins are preferred for sLNP binding (Figure 4B). Around 27.8% proteins have a PI > 7.4, suggesting that apart from the electrostatic interactions, some other types of supramolecular interactions are involved for nonspecific protein binding, such as hydrogen-bonding and hydrophobic interactions. Next, the molecular weights of corona proteins were analyzed (Figure 4C). It was found that proteins with a molecular weight less than 100 kDa constitute ca. 80.8% of the corona, and most of the enriched proteins (abundance of ~25.7%) are in the range of 40–60 kDa. Finally, the corona proteins were further categorized according to their biological functions (Figure 4D). Complement proteins (ca. 30.9%) and coagulation proteins (ca. 29.1%) are the two most abundant in the corona, followed by lipoproteins (ca. 13.4%) and immunoglobulins (ca. 2.9%). Furthermore, the top 20 most abundant corona proteins—which constitute around 72.2% of the corona - were summarized, along with their molecular weight, PI, and average abundance (Table S1). A comparison between sLNP protein corona with previously reported LNPs' corona revealed that certain protein species (e.g., fibrinogens, apolipoproteins, fibronectin, vitronectin, and complement proteins) were commonly shared between these lung-targeting LNPs.<sup>33,41,54</sup> Previous studies suggested that vitronectin might play important roles in the internalization of LNPs by lung cells.

Particularly, the *in vitro* vitronectin-coating augmented cell transfection in  $\alpha_v\beta_3$  integrin-expressing cell lines.<sup>41,54,57</sup> It is noteworthy that alpha-1-antitrypsin (AAT) is one of the top protein species enriched in the sLNP corona (Table S1). Considering the protective function of AAT in the lungs and the fact that AAT can be internalized by lung endothelial cells via endocytosis, the role of AAT in mediating sLNP lung targeting merits further investigation.<sup>58</sup>

Safety and biocompatibility are critical parameters in evaluating the translational potential of an mRNA delivery system.<sup>59,60</sup> A recent study revealed that the cationic LNP formulation incorporated with DOTAP induced thrombosis in the lung and other organs.<sup>61</sup> We first examined the possible local inflammation reaction in the lungs induced by mRNA/sLNP. The bronchoalveolar lavage fluid (BALF) was collected from Balb/c mice receiving mRNA/DOSEH. Similar numbers of macrophages in BALF were found in the PBS- and mRNA/sLNP-treated mice (Figure 5A and B), and no neutrophil was observed. The mRNA/sLNP did not result in significant variation in major cytokine expression (i.e., TNF- $\alpha$ , IL-1 $\beta$  and IL-6; Figure 5C). Furthermore, no significant difference in total protein concentration was observed (Figure 5D). These results suggested that the mRNA/sLNP did not induce obvious lung inflammation. Next, the potential hematological toxicity was examined. The total counts of red blood cells (RBCs; Figure 5E), white blood cells (WBCs; Figure 5F), lymphocytes, monocytes, and neutrophils (Figure 5G) in blood collected from mRNA/sLNP-treated mice showed no significant difference compared to the PBS-treated control group. Furthermore, both the mRNA/sLNP and PBS-treated groups possessed similar WBC differentials (Figure 5H). Next, the mouse body weight was monitored continuously for 5 days, and both mRNA/sLNP and PBS-treated mice showed a negligible body weight variation in the time course of this study (Figure S9A). No obvious clinical signs of toxicity were recorded (e.g., impeded movement, aberrant behavior, etc.). The potential hepatotoxicity and nephrotoxicity were evaluated by measuring the blood concentrations of AST (Figure 5G) and ALT (Figure S9B), urea (Figure 5H), and creatinine (Figure S9C), and no severe toxicity to the liver or kidney was observed. Finally, a histologic examination of major organs was conducted via hematoxylin and eosin (H&E) staining (Figure 5I). Comparable to the PBS group, there were no apparent morphological alterations or tissue damage observed in the mRNA/sLNP-treated group. These results underscored the biocompatibility and safety of the sLNP system.

In summary, we first synthesized sulfonium lipids (i.e., DHSEH and DOSEH), fabricated sLNPs through self-assembly, and demonstrated their application in mediating systemic delivery of mRNA to the lungs in adult mice. The sLNP-enabled, systemic, lung-specific mRNA delivery led to a uniform protein expression in all lung lobes, and it outperformed lung-tropic MC3-DOTAP formulation in terms of delivery efficacy and organ specificity. The kinetics study revealed that a higher dose induced greater and prolonged protein production. In the A14 mouse model, around 67.0% endothelial cells, 11.3% epithelial cells, and 3.5% immune cells in the lungs were transfected by mRNA/sLNP. Proteomic analysis of the sLNP protein corona shed light on the molecular mechanism of lung-targeting property, in which the fibrinogen, vitronectin, and/or AAT-mediated cell recognition and receptor-mediated internalization might be involved. The

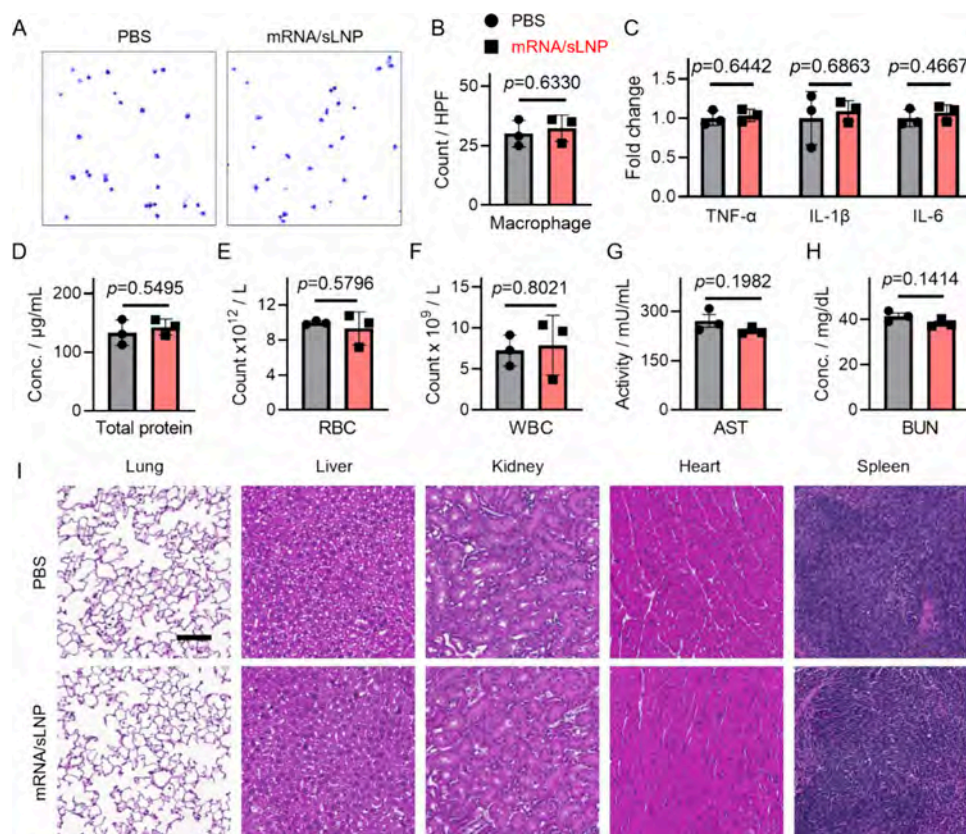


**Figure 5.** sLNP does not induce inflammation or toxicity in mice. (A) Representative images of cells collected in BALF. (B) Quantification of macrophage counts, (C) variations in cytokine levels, and (D) total protein concentration in BALF. Cell counts of (E) red blood cell (RBC) and (F) white blood cell (WBC). Quantification of (G) AST and (H) BUN in serum. Data are presented as mean  $\pm$  s.d.,  $n = 3$ , two-tailed unpaired  $t$  test. (I) H&E staining images of major organ slices. Scale bar = 100  $\mu\text{m}$ .

newly developed sLNP did not induce inflammation in the lung tissues, and no obvious toxicity to the lung, blood system, liver, kidney, heart, and spleen was observed. Collectively, these findings demonstrate that the sLNP can serve as a new class of carrier system for systemic delivery of mRNA to the lungs. We have demonstrated that nonconventional sulfonium lipid-based nanoparticles can efficiently complex with mRNA and facilitate *in vivo* delivery in an organ-specific manner. By leveraging the novel structure of sulfonium moiety, we successfully expanded the diversity of lipid chemistry available for designing lung-specific LNPs. Our ongoing efforts are focused on further optimizing and refining the sLNP formulation, as well as incorporating functional mRNA for therapeutic applications aimed at treating lung-associated diseases. Furthermore, investigation of the nanobio interactions will help deepen our understanding of the biological effects of the sLNP formulations.

## ■ ASSOCIATED CONTENT

### SI Supporting Information

The Supporting Information is available free of charge at <https://pubs.acs.org/doi/10.1021/acs.nanolett.4c01854>.

Materials and Methods, proteomics data,  $^1\text{H}$  NMR and MS spectra, bioluminescence images, DLS characterization, encapsulation efficacy, cryoEM images, FACS gating strategy, and *in vivo* toxicity study (PDF)

## ■ AUTHOR INFORMATION

### Corresponding Author

Yamin Li – Department of Pharmacology, State University of New York, Upstate Medical University, Syracuse, New York 13210, United States; [orcid.org/0000-0002-5535-1807](https://orcid.org/0000-0002-5535-1807); Email: [liyam@upstate.edu](mailto:liyam@upstate.edu)

### Authors

David O. Popoola – Department of Pharmacology, State University of New York, Upstate Medical University, Syracuse, New York 13210, United States

Zhi Cao – Department of Pharmacology, State University of New York, Upstate Medical University, Syracuse, New York 13210, United States

Yuqin Men – Department of Pharmacology, State University of New York, Upstate Medical University, Syracuse, New York 13210, United States

Xinyuan Li – Department of Pharmacology, State University of New York, Upstate Medical University, Syracuse, New York 13210, United States

Mariano Viapiano – Department of Neuroscience and Physiology, State University of New York, Upstate Medical University, Syracuse, New York 13210, United States

Stephan Wilkens – Department of Biochemistry and Molecular Biology, State University of New York, Upstate Medical University, Syracuse, New York 13210, United States

Juntao Luo – Department of Pharmacology, State University of New York, Upstate Medical University, Syracuse, New York 13210, United States

York 13210, United States; [orcid.org/0000-0002-3538-9453](https://orcid.org/0000-0002-3538-9453)

**Yong Teng** – Department of Hematology and Medical Oncology, Winship Cancer Institute, Emory University, Atlanta, Georgia 30322, United States

**Qinghe Meng** – Department of Surgery, State University of New York, Upstate Medical University, Syracuse, New York 13210, United States

Complete contact information is available at:

<https://pubs.acs.org/10.1021/acs.nanolett.4c01854>

### Author Contributions

<sup>#</sup>D.O.P. and Z.C. contributed equally. Y.L. conceived and designed this study. D.O.P., Z.C., Y.M., X.L., M.V., S.W., J.L., Y.T., Q.M., and Y.L. performed experiments. D.P., Z.C., Y.M., Q.M., and Y.L. analyzed data. All authors discussed and commented on the results. Y.L. wrote and D.P. and Y.M. revised the manuscript. All authors read, commented on, and approved the manuscript. Y.L. acquired funding and supervised the project.

### Notes

The authors declare the following competing financial interest(s): A patent application for the lipid nanoparticle materials developed in this study has been filed by the State University of New York.

### ACKNOWLEDGMENTS

We thank Dr. Dandan Guo and Changying Shi for their assistance with material characterization, Drs. Jennifer Moffat, Megan Lloyd, Somanath Kundu, and Abigail Venskus for bioluminescence imaging, Dr. Adam Waickman and Lisa Phelps for flow cytometry analysis, Drs. Jushuo Wang and Arvydas Matiukas for confocal imaging, and Ebbing De Jong for proteomics analysis. We thank Drs. Robert Cooney and Guirong Wang for helpful discussion. We thank the SUNY ESF Analytical and Technical Services, SUNY Upstate Medical University Research Flow Core, and the Department of Laboratory Animal Resources. Some elements in Figures <sup>1</sup>A, <sup>2</sup>A and <sup>3</sup>A were created by BioRender.com. Y.L. acknowledges the start-up fund from the SUNY Upstate Medical University and National Institutes of Health Grant R03EB032579.

### REFERENCES

- (1) Rohner, E.; Yang, R.; Foo, K. S.; Goedel, A.; Chien, K. R. Unlocking the promise of mRNA therapeutics. *Nat. Biotechnol.* **2022**, *40* (11), 1586–1600.
- (2) Sahin, U.; Kariko, K.; Tureci, O. mRNA-based therapeutics—developing a new class of drugs. *Nat. Rev. Drug Discov* **2014**, *13* (10), 759–80.
- (3) Hou, X.; Zaks, T.; Langer, R.; Dong, Y. Lipid nanoparticles for mRNA delivery. *Nat. Rev. Mater.* **2021**, *6* (12), 1078–1094.
- (4) Paunovska, K.; Loughrey, D.; Dahlman, J. E. Drug delivery systems for RNA therapeutics. *Nat. Rev. Genet* **2022**, *23* (5), 265–280.
- (5) Wang, C.; Zhang, Y.; Dong, Y. Lipid Nanoparticle-mRNA Formulations for Therapeutic Applications. *Acc. Chem. Res.* **2021**, *54* (23), 4283–4293.
- (6) Ye, Z.; Harmon, J.; Ni, W.; Li, Y.; Wich, D.; Xu, Q. The mRNA Vaccine Revolution: COVID-19 Has Launched the Future of Vaccinology. *ACS Nano* **2023**, *17* (16), 15231–15253.
- (7) Kon, E.; Ad-El, N.; Hazan-Halevy, I.; Stotsky-Oterin, L.; Peer, D. Targeting cancer with mRNA-lipid nanoparticles: key considerations and future prospects. *Nat. Rev. Clin Oncol* **2023**, *20* (11), 739–754.

- (8) Loughrey, D.; Dahlman, J. E. Non-liver mRNA Delivery. *Acc. Chem. Res.* **2022**, *55* (1), 13–23.
- (9) Chaudhary, N.; Newby, A. N.; Whitehead, K. A. Non-Viral RNA Delivery During Pregnancy: Opportunities and Challenges. *Small* **2023**, No. e2306134.
- (10) Kim, J.; Eygeris, Y.; Ryals, R. C.; Jozic, A.; Sahay, G. Strategies for non-viral vectors targeting organs beyond the liver. *Nat. Nanotechnol* **2024**, *19*, 428–447.
- (11) Patel, S. K.; Billingsley, M. M.; Mukalel, A. J.; Thatte, A. S.; Hamilton, A. G.; Gong, N.; El-Mayta, R.; Safford, H. C.; Merolle, M.; Mitchell, M. J. Bile acid-containing lipid nanoparticles enhance extrahepatic mRNA delivery. *Theranostics* **2024**, *14* (1), 1–16.
- (12) Han, X.; Zhang, H.; Butowska, K.; Swingle, K. L.; Alameh, M. G.; Weissman, D.; Mitchell, M. J. An ionizable lipid toolbox for RNA delivery. *Nat. Commun.* **2021**, *12* (1), 7233.
- (13) Sahu, L.; Haque, A.; Weidensee, B.; Weinmann, P.; Kormann, M. S. D. Recent Developments in mRNA-Based Protein Supplementation Therapy to Target Lung Diseases. *Mol. Ther* **2019**, *27* (4), 803–823.
- (14) Roh, E. H.; Fromen, C. A.; Sullivan, M. O. Inhalable mRNA vaccines for respiratory diseases: a roadmap. *Curr. Opin Biotechnol* **2022**, *74*, 104–109.
- (15) Lokugamage, M. P.; Vanover, D.; Beyersdorf, J.; Hatit, M. Z. C.; Rotolo, L.; Echeverri, E. S.; Peck, H. E.; Ni, H.; Yoon, J. K.; Kim, Y.; Santangelo, P. J.; Dahlman, J. E. Optimization of lipid nanoparticles for the delivery of nebulized therapeutic mRNA to the lungs. *Nat. Biomed Eng.* **2021**, *5* (9), 1059–1068.
- (16) Liu, C.; Shi, Q.; Huang, X.; Koo, S.; Kong, N.; Tao, W. mRNA-based cancer therapeutics. *Nat. Rev. Cancer* **2023**, *23* (8), 526–543.
- (17) Zhao, G.; Xue, L.; Geisler, H. C.; Xu, J.; Li, X.; Mitchell, M. J.; Vaughan, A. E. Precision treatment of viral pneumonia through macrophage-targeted lipid nanoparticle delivery. *Proc. Natl. Acad. Sci. U. S. A.* **2024**, *121* (7), No. e2314747121.
- (18) Jiang, A. Y.; Witten, J.; Raji, I. O.; Eweje, F.; MacIsaac, C.; Meng, S.; Oladimeji, F. A.; Hu, Y.; Manan, R. S.; Langer, R.; Anderson, D. G. Combinatorial development of nebulized mRNA delivery formulations for the lungs. *Nat. Nanotechnol* **2024**, *19*, 364–375.
- (19) Patel, A. K.; Kaczmarek, J. C.; Bose, S.; Kauffman, K. J.; Mir, F.; Heartlein, M. W.; DeRosa, F.; Langer, R.; Anderson, D. G. Inhaled Nanoformulated mRNA Polyplexes for Protein Production in Lung Epithelium. *Adv. Mater.* **2019**, *31* (8), No. e1805116.
- (20) Yan, Y.; Xiong, H.; Zhang, X.; Cheng, Q.; Siegwart, D. J. Systemic mRNA Delivery to the Lungs by Functional Polyester-based Carriers. *Biomacromolecules* **2017**, *18* (12), 4307–4315.
- (21) Kaczmarek, J. C.; Patel, A. K.; Kauffman, K. J.; Fenton, O. S.; Webber, M. J.; Heartlein, M. W.; DeRosa, F.; Anderson, D. G. Polymer-Lipid Nanoparticles for Systemic Delivery of mRNA to the Lungs. *Angew. Chem., Int. Ed. Engl.* **2016**, *55* (44), 13808–13812.
- (22) Tang, Z.; You, X.; Xiao, Y.; Chen, W.; Li, Y.; Huang, X.; Liu, H.; Xiao, F.; Liu, C.; Koo, S.; Kong, N.; Tao, W. Inhaled mRNA nanoparticles dual-targeting cancer cells and macrophages in the lung for effective transfection. *Proc. Natl. Acad. Sci. U. S. A.* **2023**, *120* (44), No. e2304966120.
- (23) Li, Q.; Chan, C.; Peterson, N.; Hanna, R. N.; Alfaro, A.; Allen, K. L.; Wu, H.; Dall'Acqua, W. F.; Borrok, M. J.; Santos, J. L. Engineering Caveolae-Targeted Lipid Nanoparticles To Deliver mRNA to the Lungs. *ACS Chem. Biol.* **2020**, *15* (4), 830–836.
- (24) Sung, J. C.; Pulliam, B. L.; Edwards, D. A. Nanoparticles for drug delivery to the lungs. *Trends Biotechnol* **2007**, *25* (12), 563–70.
- (25) Thakur, A. K.; Chellappan, D. K.; Dua, K.; Mehta, M.; Satija, S.; Singh, I. Patented therapeutic drug delivery strategies for targeting pulmonary diseases. *Expert Opin Ther Pat* **2020**, *30* (5), 375–387.
- (26) Sago, C. D.; Lokugamage, M. P.; Loughrey, D.; Lindsay, K. E.; Hincapie, R.; Krupczak, B. R.; Kalathoor, S.; Sato, M.; Echeverri, E. S.; Fitzgerald, J. P.; Gan, Z.; Gamboa, L.; Paunovska, K.; Sanhueza, C. A.; Hatit, M. Z. C.; Finn, M. G.; Santangelo, P. J.; Dahlman, J. E. Augmented lipid-nanoparticle-mediated in vivo genome editing in the

lungs and spleen by disrupting Cas9 activity in the liver. *Nat. Biomed Eng.* **2022**, *6* (2), 157–167.

(27) Xue, L.; Hamilton, A. G.; Zhao, G.; Xiao, Z.; El-Mayta, R.; Han, X.; Gong, N.; Xiong, X.; Xu, J.; Figueroa-Espada, C. G.; Shepherd, S. J.; Mukalel, A. J.; Alameh, M. G.; Cui, J.; Wang, K.; Vaughan, A. E.; Weissman, D.; Mitchell, M. J. High-throughput barcoding of nanoparticles identifies cationic, degradable lipid-like materials for mRNA delivery to the lungs in female preclinical models. *Nat. Commun.* **2024**, *15* (1), 1884.

(28) Wei, T.; Sun, Y.; Cheng, Q.; Chatterjee, S.; Traylor, Z.; Johnson, L. T.; Coquelin, M. L.; Wang, J.; Torres, M. J.; Lian, X.; Wang, X.; Xiao, Y.; Hodges, C. A.; Siegwart, D. J. Lung SORT LNPs enable precise homology-directed repair mediated CRISPR/Cas genome correction in cystic fibrosis models. *Nat. Commun.* **2023**, *14* (1), 7322.

(29) Kaczmarek, J. C.; Kauffman, K. J.; Fenton, O. S.; Sadtler, K.; Patel, A. K.; Heartlein, M. W.; DeRosa, F.; Anderson, D. G. Optimization of a Degradable Polymer-Lipid Nanoparticle for Potent Systemic Delivery of mRNA to the Lung Endothelium and Immune Cells. *Nano Lett.* **2018**, *18* (10), 6449–6454.

(30) Kaczmarek, J. C.; Patel, A. K.; Rhym, L. H.; Palmiero, U. C.; Bhat, B.; Heartlein, M. W.; DeRosa, F.; Anderson, D. G. Systemic delivery of mRNA and DNA to the lung using polymer-lipid nanoparticles. *Biomaterials* **2021**, *275*, No. 120966.

(31) Cheng, Q.; Wei, T.; Farbiak, L.; Johnson, L. T.; Dilliard, S. A.; Siegwart, D. J. Selective organ targeting (SORT) nanoparticles for tissue-specific mRNA delivery and CRISPR-Cas gene editing. *Nat. Nanotechnol.* **2020**, *15* (4), 313–320.

(32) LoPresti, S. T.; Arral, M. L.; Chaudhary, N.; Whitehead, K. A. The replacement of helper lipids with charged alternatives in lipid nanoparticles facilitates targeted mRNA delivery to the spleen and lungs. *J. Controlled Release* **2022**, *345*, 819–831.

(33) Qiu, M.; Tang, Y.; Chen, J.; Muriph, R.; Ye, Z.; Huang, C.; Evans, J.; Henske, E. P.; Xu, Q. Lung-selective mRNA delivery of synthetic lipid nanoparticles for the treatment of pulmonary lymphangioleiomyomatosis. *Proc. Natl. Acad. Sci. U. S. A.* **2022**, *119* (8), No. e2116271119.

(34) Eygeris, Y.; Gupta, M.; Kim, J.; Sahay, G. Chemistry of Lipid Nanoparticles for RNA Delivery. *Acc. Chem. Res.* **2022**, *55* (1), 2–12.

(35) Kulkarni, J. A.; Witzigmann, D.; Leung, J.; Tam, Y. Y. C.; Cullis, P. R. On the role of helper lipids in lipid nanoparticle formulations of siRNA. *Nanoscale* **2019**, *11* (45), 21733–21739.

(36) Li, Y.; Ye, Z.; Yang, H.; Xu, Q. Tailoring combinatorial lipid nanoparticles for intracellular delivery of nucleic acids, proteins, and drugs. *Acta Pharm. Sin B* **2022**, *12* (6), 2624–2639.

(37) Huang, Y.; Wu, J.; Li, S.; Liu, Z.; Li, Z.; Zhou, B.; Li, B. Quaternization drives spleen-to-lung tropism conversion for mRNA-loaded lipid-like nanoassemblies. *Theranostics* **2024**, *14* (2), 830–842.

(38) Majeti, B. K.; Singh, R. S.; Yadav, S. K.; Bathula, S. R.; Ramakrishna, S.; Diwan, P. V.; Madhavendra, S. S.; Chaudhuri, A. Enhanced intravenous transgene expression in mouse lung using cyclic-head cationic lipids. *Chem. Biol.* **2004**, *11* (4), 427–37.

(39) Bragonzi, A.; Dina, G.; Villa, A.; Calori, G.; Biffi, A.; Bordignon, C.; Assael, B. M.; Conese, M. Biodistribution and transgene expression with nonviral cationic vector/DNA complexes in the lungs. *Gene Ther.* **2000**, *7* (20), 1753–60.

(40) Gueguen, C.; Ben Chimol, T.; Briand, M.; Renaud, K.; Seiler, M.; Ziesel, M.; Erbacher, P.; Hellal, M. Evaluating how cationic lipid affects mRNA-LNP physical properties and biodistribution. *Eur. J. Pharm. Biopharm.* **2024**, *195*, No. 114077.

(41) Dilliard, S. A.; Cheng, Q.; Siegwart, D. J. On the mechanism of tissue-specific mRNA delivery by selective organ targeting nanoparticles. *Proc. Natl. Acad. Sci. U. S. A.* **2021**, *118* (52), No. e2109256118.

(42) Sun, H.; Zhang, Y.; Wang, J.; Su, J.; Zhou, D.; Yu, X.; Xu, Y.; Yang, W. Application of Lung-Targeted Lipid Nanoparticle-delivered mRNA of soluble PD-L1 via SORT Technology in Acute Respiratory Distress Syndrome. *Theranostics* **2023**, *13* (14), 4974–4992.

(43) Wang, X.; Liu, S.; Sun, Y.; Yu, X.; Lee, S. M.; Cheng, Q.; Wei, T.; Gong, J.; Robinson, J.; Zhang, D.; Lian, X.; Basak, P.; Siegwart, D. J. Preparation of selective organ-targeting (SORT) lipid nanoparticles (LNPs) using multiple technical methods for tissue-specific mRNA delivery. *Nat. Protoc.* **2023**, *18* (1), 265–291.

(44) Betzer, O.; Shilo, M.; Opochninsky, R.; Barnoy, E.; Motiei, M.; Okun, E.; Yadid, G.; Popovtzer, R. The effect of nanoparticle size on the ability to cross the blood-brain barrier: an in vivo study. *Nanomedicine (Lond)* **2017**, *12* (13), 1533–1546.

(45) Longmire, M.; Choyke, P. L.; Kobayashi, H. Clearance properties of nano-sized particles and molecules as imaging agents: considerations and caveats. *Nanomedicine (Lond)* **2008**, *3* (5), 703–17.

(46) Sun, Q.; Zhou, Z.; Qiu, N.; Shen, Y. Rational Design of Cancer Nanomedicine: Nanoproperty Integration and Synchronization. *Adv. Mater.* **2017**, *29* (14), No. 1606628.

(47) Euliss, L. E.; DuPont, J. A.; Gratton, S.; DeSimone, J. Imparting size, shape, and composition control of materials for nanomedicine. *Chem. Soc. Rev.* **2006**, *35* (11), 1095–104.

(48) Allen, T. M.; Cullis, P. R. Liposomal drug delivery systems: from concept to clinical applications. *Adv. Drug Deliv. Rev.* **2013**, *65* (1), 36–48.

(49) Kulkarni, J. A.; Darjuan, M. M.; Mercer, J. E.; Chen, S.; van der Meel, R.; Thewalt, J. L.; Tam, Y. Y. C.; Cullis, P. R. On the Formation and Morphology of Lipid Nanoparticles Containing Ionizable Cationic Lipids and siRNA. *ACS Nano* **2018**, *12* (5), 4787–4795.

(50) Southam, D. S.; Dolovich, M.; O'Byrne, P. M.; Inman, M. D. Distribution of intranasal instillations in mice: effects of volume, time, body position, and anesthesia. *Am. J. Physiol. Lung Cell Mol. Physiol.* **2002**, *282* (4), L833–9.

(51) Hasegawa-Baba, Y.; Kubota, H.; Takata, A.; Miyagawa, M. Intratracheal instillation methods and the distribution of administered material in the lung of the rat. *J. Toxicol. Pathol.* **2014**, *27* (3–4), 197–204.

(52) Santry, L. A.; Ingraio, J. C.; Yu, D. L.; de Jong, J. G.; van Lieshout, L. P.; Wood, G. A.; Wootton, S. K. AAV vector distribution in the mouse respiratory tract following four different methods of administration. *BMC Biotechnol.* **2017**, *17* (1), 43.

(53) Li, Y.; Jarvis, R.; Zhu, K.; Glass, Z.; Ogurlu, R.; Gao, P.; Li, P.; Chen, J.; Yu, Y.; Yang, Y.; Xu, Q. Protein and mRNA Delivery Enabled by Cholesteryl-Based Biodegradable Lipidoid Nanoparticles. *Angew. Chem., Int. Ed. Engl.* **2020**, *59* (35), 14957–14964.

(54) Cao, Y.; He, Z.; Chen, Q.; He, X.; Su, L.; Yu, W.; Zhang, M.; Yang, H.; Huang, X.; Li, J. Helper-Polymer Based Five-Element Nanoparticles (FNPs) for Lung-Specific mRNA Delivery with Long-Term Stability after Lyophilization. *Nano Lett.* **2022**, *22* (16), 6580–6589.

(55) Li, Y. X.; Wang, H. B.; Li, J.; Jin, J. B.; Hu, J. B.; Yang, C. L. Targeting pulmonary vascular endothelial cells for the treatment of respiratory diseases. *Front Pharmacol.* **2022**, *13*, No. 983816.

(56) Nienhaus, K.; Nienhaus, G. U. Mechanistic Understanding of Protein Corona Formation around Nanoparticles: Old Puzzles and New Insights. *Small* **2023**, *19* (28), No. e2301663.

(57) Caracciolo, G.; Cardarelli, F.; Pozzi, D.; Salomone, F.; Maccari, G.; Bardi, G.; Capriotti, A. L.; Cavaliere, C.; Papi, M.; Lagana, A. Selective targeting capability acquired with a protein corona adsorbed on the surface of 1,2-dioleoyl-3-trimethylammonium propane/DNA nanoparticles. *ACS Appl. Mater. Interfaces* **2013**, *5* (24), 13171–9.

(58) Kalfopoulos, M.; Wetmore, K.; ElMallah, M. K. Pathophysiology of Alpha-1 Antitrypsin Lung Disease. *Methods in Molecular Biology* **2017**, *1639*, 9–19.

(59) Bitounis, D.; Jacquinet, E.; Rogers, M. A.; Amiji, M. M. Strategies to reduce the risks of mRNA drug and vaccine toxicity. *Nat. Rev. Drug Discov.* **2024**, *23*, 281–300.

(60) Qiu, M.; Li, Y.; Bloomer, H.; Xu, Q. Developing Biodegradable Lipid Nanoparticles for Intracellular mRNA Delivery and Genome Editing. *Acc. Chem. Res.* **2021**, *54* (21), 4001–4011.

(61) Omo-Lamai, S.; Zamora, M. E.; Patel, M. N.; Wu, J.; Nong, J.; Wang, Z.; Peshkova, A.; Majumder, A.; Melamed, J. R.; Chase, L. S.;

Essien, E. O.; Weissman, D.; Muzykantov, V. R.; Marcos-Contreras, O. A.; Myerson, J. W.; Brenner, J. S. Physicochemical Targeting of Lipid Nanoparticles to the Lungs Induces Clotting: Mechanisms and Solutions. *Adv. Mater.* **2024**, No. e2312026.